
HyperTokens: Controlling Token Dynamics for Continual Video–Language Understanding

Toan Nguyen¹ Yang Liu¹ Celso De Melo² Flora D. Salim¹

Abstract

Continual VideoQA with multimodal LLMs is hindered by interference between tasks and the prohibitive cost of storing task-specific prompts. We introduce HyperTokens, a transformer-based token generator that produces fine-tuning tokens on demand, giving explicit control over prompt updates while keeping memory fixed. To suppress forgetting, we propose meta-inspired regularisers that look ahead to avoid task-specific sharp directions and anchor the evolving generator to prior tasks. We further connect our objective to sharpness-aware optimisation, providing insight into why it encourages flatter cross-task minima and improves retention. Beyond regularisation, HyperTokens exploits lightweight auxiliary multimodal supervision through shared generation weights; guided by a causal perspective, we design feasible objectives and surrogate mutual-information losses to regularise anti-causal cross-modal directions. Across two standard continual VideoQA benchmarks, HyperTokens achieves higher average accuracy with substantially lower forgetting. Finally, we introduce a challenging cross-modal ImageQA→VideoQA protocol and show that HyperTokens enables robust continual transfer in this setting.

1. Introduction

Modern multimodal LLMs are increasingly deployed on continuous multimodal streams of video, audio, and language from dynamic environments (e.g., wearables, cameras, and sensors), driven by their remarkable ability to learn and reason over multimodal structure, as evidenced by strong performance on VideoQA (Shu et al., 2025; Maaz et al., 2024; Qian et al., 2024). In such settings, the con-

ventional *train-then-deploy* paradigm for large-scale pre-trained models (Liu et al., 2024a; Team et al., 2024; Zhao et al., 2024; Liu et al., 2025b) hinges on stationarity, and can degrade when confronted with evolving tasks, distribution shifts, and previously unseen concepts. Naïvely fine-tuning on new tasks often causes *catastrophic forgetting* (McCloskey & Cohen, 1989; Cai et al., 2024), which overwrites prior knowledge, and the problem compounds as tasks accumulate; moreover, updating all parameters of a large pretrained model is computationally expensive and quickly becomes impractical. A practical alternative is *parameter-efficient adaptation* (PEA) (Cai et al., 2024; Adhikari et al., 2025; Razdaibiedina et al., 2023), which updates only a small set of added parameters on top of a frozen backbone to accommodate incoming data while largely preserving the model’s base knowledge.

However, in continual learning for challenging multimodal video tasks such as VideoQA, task distributions can differ sharply (e.g., indoor versus outdoor videos or distinct question types), so prompt updates may interfere and still incur substantial forgetting without careful parameter control (Tan et al., 2025a). Recent methods (Razdaibiedina et al., 2023; Rusu et al., 2016) sidestep this by storing task-specific adapter prompts and stacking them over time, but the approach scales poorly as the number of tasks grows. Other approaches (Tan et al., 2025a; Cai et al., 2024; Wang et al., 2022b) share a prompt parameterisation across tasks, but updates can conflict on the shared components and trigger interference under a small prompt budget. Alternatives such as LoRA or prefix tuning (Adhikari et al., 2025; Yu et al., 2025) are efficient, yet they remain challenging to (i) scale *nicely* to many tasks, (ii) preserve fine-grained, task-specific control *without* cross-task interference, and (iii) extend reliably to multimodal VideoQA.

To address these challenges, we draw inspiration from hypernetworks (Ha et al., 2017) and propose **HyperTokens**, a universal token generator that produces adapter tokens *on demand*. Given a compact multimodal task code, HyperTokens synthesises task-specific prompts while keeping the size of generator fixed, so memory grows only minimally with the number of tasks. Figure 1 illustrates the design. A key challenge in hypernetwork-based prompt

¹School of Computer Science and Engineering, University of New South Wales, Australia ²DEVCOM Army Research Laboratory, USA. Correspondence to: Flora D. Salim <flora.salim@unsw.edu.au>.

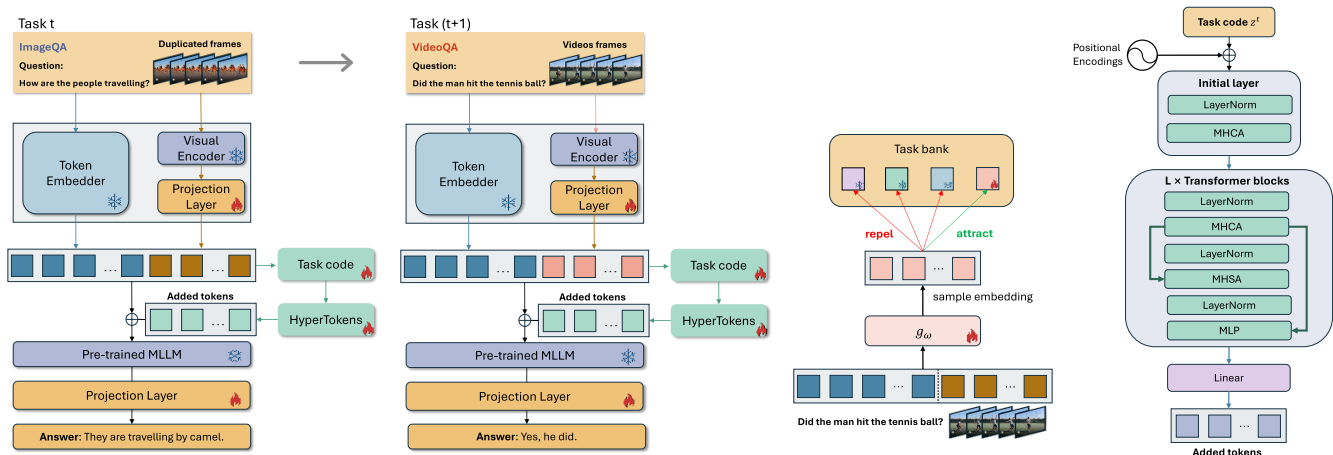


Figure 1: **HyperTokens overview.** (Left) Continual adaptation with HyperTokens for VideoQA and cross-modal transfer VisualQA→VideoQA. A fixed-size generator synthesises task-specific fine-tuning tokens. (Middle) Task-code learning via a multimodal contrastive objective with a prototype bank. (Right) Transformer-based token-generator architecture.

control is to learn informative task codes and to update the token generator without forgetting. To learn task codes, we introduce a contrastive embedding loss that leverages both video and question features to capture task-specific structure. To preserve the generator, we use a transformer-based token generator trained with a meta-inspired objective that (i) *looks ahead* to avoid task-specific overfitting directions and (ii) *looks back* to match an anchored behaviour given a small set of past task codes. We theoretically connect this objective to sharpness-aware minimisation (SAM) (Foret et al., 2021), showing that it favours flatter cross-task minima and improves robustness under continual adaptation.

Beyond regularisation, HyperTokens benefits from lightweight auxiliary multimodal supervision effectively enabled by shared generation weights. From a causal view (Pearl, 2009; Nguyen et al., 2023) of VideoQA, we prioritise feasible objectives that follow at least one causal direction (e.g., predicting questions from videos and answers), since the reverse direction (predicting videos from questions and answers) is *anti-causal* and prone to hallucinated visual evidence. To still exploit this signal, we introduce surrogate mutual-information losses (Oord et al., 2018) at both the token and global video levels to regularise cross-modal alignment. Empirically, HyperTokens achieves strong accuracy with substantially reduced forgetting on standard continual VideoQA benchmarks. Further, we introduce a new and highly challenging ImageQA→VideoQA setting, where the model continually shift from static image understanding to temporal video reasoning. This transfer induces both a *modality mismatch* and a *learning-nature mismatch* (single-frame recognition and temporal reasoning), under which recent SOTA PEA baselines degrade significantly;

in contrast, HyperTokens remains robust and surpasses the strongest prior method, underscoring the effectiveness of multimodal token-hypernetwork generation.

2. Related Work

Video Question Answering (VideoQA) aims to strengthen video–language understanding by requiring models to answer questions grounded in video inputs. Existing approaches either develop specialised video vision–language models (Deitke et al., 2025; Alayrac et al., 2022; Yu et al., 2023) or adapt large pretrained LLMs to better capture temporal visual context (Yang et al., 2022; Zhang et al., 2024a;b). However, none of these methods is designed for continual learning from a stream of VideoQA datasets, where the input distribution can shift substantially.

Continual Learning for VideoQA considers a streaming setting where a model is trained sequentially on multiple VideoQA datasets; the key challenge is mitigating catastrophic forgetting. Replay-based methods alleviate forgetting by storing a small buffer of past samples to replay them while learning new tasks (Buzzega et al., 2020; Nguyen et al., 2024), but storing videos is often prohibitive. Regularisation and architectural approaches have been mainly studied for multimodal classification (Ke et al., 2020; Jha et al., 2024; Liu et al., 2025a) and do not readily transfer to next-token LLM-style VideoQA. Recent work therefore emphasises parameter-efficient adaptation, updating only a small set of added parameters atop a frozen backbone to accommodate new tasks while preserving prior knowledge.

Parameter-Efficient Adaptation (PEA) (Zhang et al., 2024b; Li & Liang, 2021) enable continual adaptation in

LLMs/VLMs by training lightweight task-specific modules while freezing the backbone, thereby preserving base knowledge. L2P (Wang et al., 2022b) maintains a prompt pool and appends retrieved prompts to the input embeddings via prompt tuning (Lester et al., 2021) for task-agnostic PEA, but the pool’s fixed capacity induces interference and forgetting. DualPrompt (Wang et al., 2022a) mitigates this by introducing prompts—task-invariant (G-Prompt) and task-specific (E-Prompt), with CODA-Prompt (Smith et al., 2023) extends this idea by attention-prompting modules. LAE (Gao et al., 2023) proposes a unified PEA framework where an adaptation-speed calibration module guides an online PEA module while consolidating knowledge into an offline PEA module, and combines the two at inference. HiDe-Prompt (Wang et al., 2023) adopts a hierarchical prompting design and uses an ensemble at inference. ProgPrompt (Razdaibiedina et al., 2023) learns task-specific prompts and concatenates them into a frozen sequence, akin to progressive networks (Rusu et al., 2016). However, its prompt bank grows linearly with the number of tasks, limiting scalability in video–text settings. AdaPrefix++ (Adhikari et al., 2025) is closest to HyperTokens, using hypernetworks (Ha et al., 2017) to generate fine-tuning parameters, but it can be seen as a *no-look-ahead* variant: it omits our look-ahead regulariser (whose gains grow with more look-ahead steps) and lacks theoretical support for its regularisation. Moreover, all above methods are evaluated in unimodal continual learning, leaving multimodal continual VideoQA largely unexplored.

On LLM-based continual VideoQA, DAM (Cheng et al., 2025) tackles domain-incremental settings with unknown target domains by merging task-specific adapters at inference. ColPro (Cai et al., 2024) improves task-aware prompting by injecting question, visual, and temporal cues into attention-stage tokens, and Bisecl (Tan et al., 2025a), inspired by neurobiology (Olsen et al., 2012), streamlines ColPro and mitigates update conflicts via contrastive prompt learning. However, their shared prompt matrices can induce cross-task interference and forgetting. Overall, most prior methods lack a scalable mechanism for task-specific prompt control in continual VideoQA. HyperTokens addresses this gap with *on-demand* task-conditioned token generation, grounded regularisation, and strong empirical results, including robust cross-modal transfer from ImageQA→VideoQA.

HyperNetworks are neural networks that output the parameters of another network conditioned on an auxiliary signal (Ha et al., 2017). In continual learning, many methods condition on task identity to synthesise full or partial model weights (von Oswald et al., 2020; Hemati et al., 2023; Chandra et al., 2023; Kumaravelu et al., 2025), which are computationally costly and poorly suited to LLMs. Adaprefix++ lowers cost by generating adapter and prefix parameters (Adhikari et al., 2025), but it still caches per-task hy-

pernetwork parameters for regularisation and learns weak multimodal task embeddings. Our *HyperTokens* introduces a meta-learning regulariser with theoretical guarantees against forgetting, learns stronger multimodal task embeddings, and generates lightweight token/LoRA parameters—enabling scalable continual adaptation. Recent hypernetwork-based LLM adaptation methods (Charakorn et al., 2025; Tan et al., 2025b) target different settings and lack our features.

3. Background

Problem Setup We study continual learning for VideoQA, where training data arrive sequentially as tasks indexed by $t = 1, \dots, T$. Each task t provides a dataset $\mathcal{D}_t = \{(V_i^t, Q_i^t, A_i^t)\}_{i=1}^{N_t}$ of video–question–answer triplets, where V_i^t is a video, Q_i^t a question, and A_i^t its answer. Our objective is to learn a *continual* vision language model (VLM) f_θ that maps a video V and question Q to an answer A (i.e., $A = f_\theta(V, Q)$), and performs well on the current task t without degrading performance on prior tasks $1, \dots, t-1$. We optimise f_θ with the standard next-token negative log-likelihood (NLL):

$$\mathcal{L}_{\text{NLL}}^t = -\mathbb{E}_i \left[\sum_{k=0}^{N_{i,a}^t - 1} \log P(a_{i,k+1}^t \mid V_i^t, Q_i^t, A_{i,\leq k}^t) \right] \quad (1)$$

where $V_i^t \in \mathbb{R}^{N_{i,v}^t \times C}$ is the video-token sequence from a pretrained ViT (Dosovitskiy et al., 2021), and $Q_i^t \in \mathbb{R}^{N_{i,q}^t \times C}$ and $A_i^t \in \mathbb{R}^{N_{i,a}^t \times C}$ are the embedded question- and answer-token sequences for sample i in task t . The lengths are $N_{i,v}^t$, $N_{i,q}^t$, and $N_{i,a}^t$; C is the model’s hidden dimension; and $A_{i,\leq k}^t$ denotes the prefix of A_i^t of length k .

Forgetting Optimising f_θ with Eq. (3) in sequence induces *forgetting*: at step t , updates ignore the cumulative past objective $\mathcal{L}_{\text{NLL}}^{\leq t-1}$ and, under rehearsal-free training, have no access to prior data or gradients. PEA methods adapt the pretrained VLM via small, task-specific modules (e.g., prompts, adapters, LoRA) while the backbone stays frozen; the modules are retained and routed at inference.

4. Method

4.1. Desiderata for continual PEA

While PEA is appealing, we argue that effective forgetting mitigation hinges on two desiderata that existing methods fail to meet in a scalable and reliable manner.

Optimal per-task control of learnable tokens. Prior work either expands task-specific tokens as tasks arrive, increasing memory and compute costs (e.g., (Razdaibiedina et al.,

2023)), or relies on shared prompt parameters that can induce cross-task interference among learnable prompts like (Tan et al., 2025a).

Auxiliary supervision for token learning. To better capture multimodal structure during fine-tuning, recent methods (Tan et al., 2025a; Cai et al., 2024) introduce two auxiliary objectives: predicting the question given the video and answer, $p(Q | V, A)$, and predicting the video given the question and answer, $p(V | Q, A)$. We argue, from a causal perspective (Pearl, 2009; Nguyen et al., 2023), that $p(Q | V, A)$ is a feasible auxiliary loss, whereas $p(V | Q, A)$ is misaligned and ineffective. Formally, a causal graph for VideoQA is: (i) the video V is a common cause of both the question Q and answer A , and (ii) the answer A depends on both the video and question, i.e., $V \rightarrow Q$, $V \rightarrow A$, and $Q \rightarrow A$. Under this structure, conditioning on (V, A) yields an informative signal for predicting Q , encouraging question-type awareness and aligning linguistic cues with visual evidence. In contrast, modelling $p(V | Q, A)$ requires reconstructing visual content from sparse text and is underdetermined—many distinct videos can correspond to the same (Q, A) . This *anti-causal* objective therefore encourages shortcut learning rather than improved grounding.

4.2. HyperTokens

To meet these desiderata, we introduce a hypernetwork (Ha et al., 2017) that generates task-specific token embeddings (**HyperTokens**) and optimises them jointly across layers, enabling stable, scalable adaptation under a nearly *fixed* parameter budget. See Fig. 1 for an overview of our method.

4.2.1. METHOD OVERVIEW

HyperTokens Generator Let H_ϕ denote a hypernetwork (parameterised by ϕ) that, given a task code $z^t \in \mathbb{R}^{N_z \times C_z}$, generates a sequence of prompt tokens for task t :

$$P_i^t = H_\phi(z^t) \in \mathbb{R}^{N_{i,p}^t \times C}, \quad (2)$$

where $N_{i,p}^t$ denotes the number of generated prompt tokens, and z^t is a *low-dimensional* task- t code with feature dimension C_z and sequence length N_z , such that $N_z C_z \ll N_{i,p}^t C$.

Training Objective Conditioned on the generated prompts P_i^t , we fine-tune the multimodal LLM on task t with

$$\mathcal{L}_{\text{NLL}}^t = -\mathbb{E}_i \left[\sum_{k=0}^{N_{i,a}^t - 1} \log P(a_{i,k+1}^t | V_i^t, Q_i^t, A_{i,\leq k}^t, P_i^t) \right] \quad (3)$$

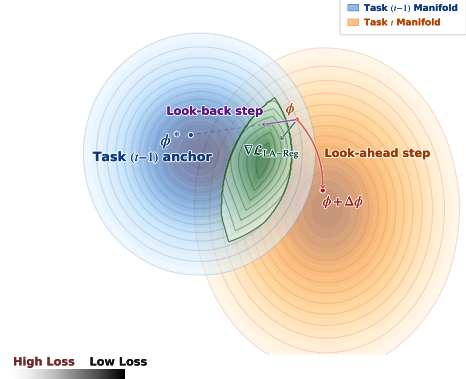


Figure 2: **Geometry of LA-Reg in optimisation space.** LA-Reg steers optimisation into the shared low-loss region (green)—a flatter minima basin across tasks—by balancing progress along the task- t direction and alignment with the task- $(t-1)$ anchor direction. Note that we regularise in the output-prompt space (not parameter space).

A key task is preventing forgetting in H_ϕ so it continues to generate correct prompts for prior tasks. A naïve approach is to store past samples and penalise changes in the generated prompts for previous tasks. However, this approach incurs substantial memory overhead, especially for VideoQA. Inspired by (Benjamin et al., 2019; von Oswald et al., 2020), we introduce **LookAhead-Regularisation (LA-Reg)**, a meta-learning regulariser that constrains drift in ϕ using only compact past task codes z^τ ($\tau < t$):

$$\mathcal{L}_{\text{LA-Reg}}^t = \sum_{\tau=1}^{t-1} \|H_{\phi^*}(z^\tau) - H_{\phi+\Delta\phi}(z^\tau)\|_2^2, \quad (4)$$

where ϕ^* are the parameters before task t , and Δ_ϕ is a *fixed look-ahead* inner-loop update obtained by taking M gradient steps on $\mathcal{L}_{\text{NLL}}^t$ with respect to H_ϕ . We then apply an outer-loop regulariser that constrains the resulting drift, balancing plasticity for task t with stability on prior tasks. In practice, $M = 2$ suffices, and our update admits efficient first-order meta-learning implementations (e.g., (Nichol et al., 2018)). Notably, (von Oswald et al., 2020) corresponds to the special case $M = 1$; in our setting, this naïve one-step look-ahead is typically insufficient unless augmented to approximate higher orders.

Learn Task Codes Each task code z^t generates a unique set of prompt tokens; we now describe how to learn it effectively. One way is to let z^t learn naturally via gradients from $\mathcal{L}_{\text{NLL}}^t$ and $\mathcal{L}_{\text{reg}}^t$. However, this may leave z_t insufficiently expressive for generating prompts. Accordingly, z^t should directly ingest both video and language signals—unlike (Tan et al., 2025a), which learns task-specific prompts from questions alone. We therefore introduce a

lightweight encoder g_ω (convolution + attention) that, for each sample (V_i^t, Q_i^t) , produces a per-sample embedding $\hat{z}_i^t = g_\omega(V_i^t, Q_i^t) \in \mathbb{R}^{N_z \times C_z}$. We then optimise z^t by aligning it with the per-sample embeddings using a contrastive task prototype loss (Fig. 1, middle):

$$\mathcal{L}_{\text{Ctr}}^t = -\mathbb{E}_i \left[\log \frac{\exp(\hat{z}_i^{t\top} \hat{z}^t / \rho)}{\sum_{\bar{z} \in \{\hat{z}^t\} \cup \mathcal{N}^t} \exp(\hat{z}_i^{t\top} \bar{z} / \rho)} \right], \quad (5)$$

where $\hat{z}_i^t = \text{Norm}(\text{Pool}(\hat{z}_i^t))$, $\hat{z}^t = \text{Norm}(\text{Pool}(z^t))$; $\mathcal{N}_{\text{Ctr}}^t$ collects negative prototypes (e.g., codes from previous tasks $\{\hat{z}^\tau\}_{\tau < t}$); and ρ is the temperature. Sharing g_ω helps initialise new tasks and capture shared knowledge, while task-specific information is preserved in the task codes z^τ .

Design H_ϕ We parameterise H_ϕ as a prompt-encoder tokeniser, inspired by ViT-style tokenisers in VLMs (Liu et al., 2024b) (Fig. 1, right). H_ϕ is a lightweight Transformer that maps a task code z^t to $N_{i,p}^t$ continuous prompt tokens in \mathbb{R}^C . We project z^t to the model width with $W_z \in \mathbb{R}^{C_z \times C}$ and add positional encodings E_{pos}^z :

$$z^t \leftarrow z^t W_z + E_{\text{pos}}^z. \quad (6)$$

We introduce learnable prompt queries $z^{q,t} \in \mathbb{R}^{N_{i,p}^t \times C}$ (positional information absorbed into $z^{q,t}$) and initialise the encoder by cross-attending queries to z^t :

$$U^{(0)} = z^{q,t} + \text{MHCA}(\text{LN}(z^{q,t}), K = z^t, V = z^t), \quad (7)$$

where MHCA is multi-head cross-attention and LN is LayerNorm. We then apply L pre-norm Transformer blocks. For $\ell = 0, \dots, L-1$:

$$\begin{aligned} U^{(\ell,c)} &= U^{(\ell)} + \text{MHCA}(\text{LN}(U^{(\ell)}), K = z^t, V = z^t), \\ U^{(\ell,s)} &= U^{(\ell,c)} + \text{MHSA}(\text{LN}(U^{(\ell,c)})), \\ U^{(\ell+1)} &= U^{(\ell,s)} + \text{MLP}(\text{LN}(U^{(\ell,s)})), \end{aligned} \quad (8)$$

where MHSA is self-attention over queries and MLP is a position-wise feed-forward network. Finally,

$$P^t = U^{(L)} W_o. \quad (9)$$

Inference Without Task Codes Since HyperTokens routes adaptation via explicit task codes, reliable inference under *unknown task identity* and *distribution shift* (e.g., continual QA moving from images to videos) requires robust task-code retrieval. We therefore stabilise the task encoder g_ω with an EWC-style weight regulariser (Kirkpatrick et al., 2017), denoted $\mathcal{L}_{\omega\text{-Reg}}$, to prevent drift while learning new tasks. Concretely, at epoch e , we penalise deviation of the current encoder parameters ω_e from the previous-task anchor ω^* :

$$\mathcal{L}_{\omega\text{-Reg}}^t = \sum_p I_p^{\text{old}} (\omega_{e,p} - \omega_k^*)^2, \quad (10)$$

where I_p^{old} is the Synaptic Intelligence (SI) importance score (Zenke et al., 2017), weighting each parameter ω_p by its relevance to past tasks. This regulariser stabilises g_ω , yielding a reliable test embedding $z_{\text{test}} = g_\omega(V_{\text{test}}, Q_{\text{test}})$ and enabling optimisation-free test-time routing via nearest-neighbour retrieval from the task bank without task IDs.

4.2.2. AUXILIARY LEARNING

Auxiliary Supervision for Question Modality. As discussed in 4.1, we introduce an auxiliary objective that models $p(Q | V, A, P)$. This loss provides an additional training signal for token learning, particularly when tasks exhibit substantial shifts in question distribution, and encourages better cross-modal interactions. We define the objective as:

$$\mathcal{L}_{\text{Ques}}^t = -\mathbb{E}_i \left[\sum_{k=0}^{N_{i,q}^t - 1} \log P(q_{i,k+1}^t | V_i^t, A_i^t, Q_{i,\leq k}^t, P_i^t) \right] \quad (11)$$

Auxiliary Supervision for Video Modality Rather than explicitly modelling the anti-causal conditional $p(V | Q, A, P)$, we promote video–QA alignment by maximising a lower bound on the mutual information $I(V; Q, A, P)$ using a retrieval-style InfoNCE objective (Oord et al., 2018). Let $S_i^t = (Q_i^t, A_i^t, P_i^t)$ denote the QA-side variables, and $V_i^t = (v_{i,1}^t, \dots, v_{i,N_{i,v}^t}^t)$ the sequence of video tokens for sample i in task t . By the chain rule of mutual information,

$$I(V_i^t; S_i^t) = \sum_{k=0}^{N_{i,v}^t - 1} I(v_{i,k+1}^t; S_i^t | v_{i,\leq k}^t). \quad (12)$$

Motivated by (12), we propose a *multi-level* contrastive objective that (i) preserves temporal predictiveness at the token level and (ii) enforces global video–QA matching at the sequence level.

Token-level predictive alignment. For each prefix index k , we encode the context $(S_i^t, v_{i,\leq k}^t)$ into an LLM hidden state $h_{i,k}^t = \text{LLM}([S_i^t; v_{i,\leq k}^t])_{\text{pos}(v_{i,k}^t)} \in \mathbb{R}^C$ and treat the next token $v_{i,k+1}^t$ as the positive target. Given a candidate set $\mathcal{C}_{i,k}^t$ containing the positive token and negatives, we adopt the standard InfoNCE objective:

$$\mathcal{L}_{\text{Tok}}^t = -\mathbb{E}_{i,k} \left[\log \frac{\exp(v_{i,k+1}^t \top h_{i,k}^t / \rho)}{\sum_{\bar{v} \in \{v_{i,k+1}^t\} \cup \mathcal{N}_{\text{Tok},i,k}^t} \exp(\bar{v} \top h_{i,k}^t / \rho)} \right]. \quad (13)$$

We form $\mathcal{N}_{\text{Tok},i,k}^t$ from within-video tokens (e.g., $\{v_{i,j}^t\}_{j=1}^{N_{i,v}^t}$), yielding hard negatives that encourage $h_{i,k}^t$ to

stay predictive of future visual tokens. This token-level term serves as a surrogate for the chain-rule decomposition in (12). However, within-video negatives are local and do not enforce *cross-video* video–text alignment, motivating the complementary video-level retrieval loss in Eq. (14).

Video-level global alignment. To complement $\mathcal{L}_{\text{Tok}}^t$, we introduce an in-batch retrieval loss that enforces *global* video–QA alignment. Let $h_{\text{qav},i}^t(k)$ denote the pooled QAV query at prefix index k , and $h_{\text{vid},j}^t(k)$ the pooled representation of video j at the same prefix. We optimise:

$$\mathcal{L}_{\text{Vid}}^t = -\mathbb{E}_{i,k} \left[\log \frac{\exp(h_{\text{qav},i}^t(k)^\top h_{\text{vid},i}^t(k)/\rho)}{\sum_{(j,k') \in \mathcal{N}_{\text{Vid},i,k}^t} \exp(h_{\text{qav},i}^t(k)^\top h_{\text{vid},j}^t(k')/\rho)} \right] \quad (14)$$

where $\mathcal{N}_{\text{Vid},i,k}^t$ contains the positive (i, k) and in-batch negatives from other videos (across prefixes).

Final loss. At task t , we optimise the following objective:

$$\mathcal{L}_{\text{Final}}^t = \mathcal{L}_{\text{NLL}}^t + \sum_{\ell \in \{\text{LA-Reg}, \text{Ctr}, \omega\text{-Reg}, \text{Aux}\}} \alpha_\ell \mathcal{L}_\ell^t, \quad (15)$$

where $\mathcal{L}_{\text{Aux}}^t = \mathcal{L}_{\text{Ques}}^t + \mathcal{L}_{\text{Tok}}^t + \mathcal{L}_{\text{Vid}}^t$. Unless otherwise specified, all three auxiliary terms are weighted equally.

4.3. Theoretical Analysis of HyperTokens

We discuss the theoretical advantages of HyperTokens that underpin their superior performance in continual learning; comprehensive proofs are provided in Appendix B.

Theorem 4.1 (LA-Reg as task-wise sharpness-aware regularisation). *Let $J_\phi(z) := \partial H_\phi(z)/\partial \phi$ denote the Jacobian of H_ϕ w.r.t. ϕ . For the current task t , define the gradient $g(\phi) := \nabla_\phi \mathcal{L}_{\text{NLL}}^t(\phi)$ and the lookahead displacement*

$$\Delta\phi := -\eta g(\phi).$$

Define the LA-Reg objective over previous tasks $\tau < t$ with stored codes z^τ and reference parameters ϕ^ by*

$$\mathcal{L}_{\text{LA-Reg}}^t(\phi) := \sum_{\tau=1}^{t-1} \|H_{\phi+\Delta\phi}(z^\tau) - H_{\phi^*}(z^\tau)\|_2^2, \quad (16)$$

(which matches Eq. 4). Assume:

(A1) (**Smooth token generator**) *For all $\tau < t$, $H_\phi(z^\tau)$ is twice continuously differentiable in ϕ and admits the expansion*

$$H_{\phi+\Delta\phi}(z^\tau) = H_\phi(z^\tau) + J_\phi(z^\tau)\Delta\phi + r_\tau,$$

where $\|r_\tau\|_2 \leq C_H \|\Delta\phi\|_2^2$ and $\|J_\phi(z^\tau)\| \leq L_J$ for constants $C_H, L_J > 0$ (with $\|\cdot\|$ the operator norm).

(A2) (**Reference proximity**) *There exists $\varepsilon \geq 0$ such that for all $\tau < t$,*

$$\|H_{\phi^*}(z^\tau) - H_\phi(z^\tau)\|_2 \leq \varepsilon.$$

(A3) (**Bounded current-task gradient**) $\|g(\phi)\|_2 = \|\nabla_\phi \mathcal{L}_{\text{NLL}}^t(\phi)\|_2 \leq G$ for some $G > 0$.

Then, for sufficiently small η , there exists a constant $C > 0$ (independent of η) such that

$$\left| \mathcal{L}_{\text{LA-Reg}}^t(\phi) - \eta^2 \sum_{\tau=1}^{t-1} \|J_\phi(z^\tau) g(\phi)\|_2^2 \right| \leq C(\varepsilon^2 + \varepsilon\eta + \eta^3). \quad (17)$$

The leading term $\eta^2 \sum_{\tau=1}^{t-1} \|J_\phi(z^\tau) g(\phi)\|_2^2$ measures how strongly past-task representations change when moving ϕ along the current-task gradient direction. Large values indicate that task t 's gradient induces large representational changes for past tasks (a ‘‘sharp’’ direction). By penalising this quantity, $\mathcal{L}_{\text{LA-Reg}}^t$ discourages such directions and instead prefers flatter updates to previous tasks, hence acting as a sharpness-aware regulariser. The theorem connects two areas: sharpness-aware generalisation (Foret et al., 2021) and continual learning.

5. Experiments

5.1. Continual VideoQA

5.1.1. SETUP

Dataset We evaluate on two widely used benchmarks: NEXT-QA (Xiao et al., 2021) and DramaQA (Choi et al., 2021). Following (Tan et al., 2025a), we partition NEXT-QA into eight sequential tasks by question type: TP, CW, DC, TC, DL, DO, TN, CH; these cover causal, descriptive, and temporal categories. For DramaQA, following (Cai et al., 2024), we split tasks by question type in the challenging order: What, Who, Where, How, Why.

Baselines We evaluate PEA baselines for LLM-based continual VideoQA: Bisecl (Tan et al., 2025a), DAM (Cheng et al., 2025), ColPro (Cai et al., 2024), ProgPrompt (Razdaibiedina et al., 2023), LAE (Gao et al., 2023), DualPrompt (Wang et al., 2022a), L2P (Wang et al., 2022b); and naive LLaMA-Adapter (Zhang et al., 2024b).

Metrics We use two metrics: **Acc** (\uparrow) and **Fog** (\downarrow). **Acc** is the mean top-1 accuracy across tasks after the sequence; **Fog** is the average drop from each task’s best accuracy to its final accuracy.

Implementation Details We use LLaMA-2-7B (Touvron et al., 2023) as the backbone LLM and CLIP ViT-L/14 (Radford et al., 2021; Dosovitskiy et al., 2021) as the visual

Table 1: Continual VideoQA results on NExT-QA and DramaQA with per-dataset accuracy and forgetting. **Bold** and underline denote the best and second-best results.

Method (Venue)	NExT-QA		DramaQA	
	Acc (↑)	Fog (↓)	Acc (↑)	Fog (↓)
LLaMA-Adapter (ICLR'24)	46.58	13.83	60.99	24.39
L2P (CVPR'22)	48.82	12.25	62.50	20.67
DualPrompt (ECCV'22)	50.62	11.74	65.89	17.93
LAE (ICCV'23)	49.38	11.47	65.82	17.35
ProgPrompt (ICLR'23)	53.95	10.69	67.92	14.95
ColPro (EMNLP'24)	55.14	7.43	71.24	12.64
DAM (WACV'25)	53.88	9.99	67.37	15.19
Bisecl (NeurIPS'25)	<u>62.37</u>	<u>5.34</u>	<u>71.49</u>	<u>10.37</u>
HyperTokens (ours)	64.75	3.62	71.62	9.84

encoder in all experiments; both are kept frozen throughout continual training. Unless otherwise stated, we use LLaMA-Adapter (Zhang et al., 2024b) with 32 adapter layers. Following (Tan et al., 2025a; Cai et al., 2024), we sample each video into 10 frames and resize them to 224×224 to extract visual features. Text sequences are truncated or padded to 128 tokens for NExT-QA, 280 for DramaQA. We fine-tune for five epochs on NExT-QA and for ten epochs on DramaQA. By default, LA-Reg uses two look-ahead steps. Full implementation details are provided in Appendix C.

5.1.2. RESULTS

Performance Comparison Table 1 shows that HyperTokens sets a new state of the art on both datasets, delivering higher **Acc** with lower **Fog**. Against Bisecl, it boosts NExT-QA accuracy by $\sim 2\%$ (averaged over 8 tasks) while cutting forgetting by $\sim 2\%$. The advantage carries over to the distinct DramaQA domain, where HyperTokens also surpasses strong prompt-based baselines (e.g., ProgPrompt), highlighting the benefit of our controlled prompt fine-tuning via multimodal hypernetworks.

Acc and Fog Changes We report **Acc** and **Fog** after each continual task on NExT-QA, and compare the fine-tuning trajectory against Bisecl in Fig. 3. HyperTokens consistently achieves higher **Acc** and lower **Fog**, with a stable 2%–5% reduction in **Fog** across all endpoints over the 8-task sequence.

5.1.3. ANALYSIS AND ABLATION STUDIES

Token Analysis We examine how task-specific tokens evolve under continual adaptation by visualising their representations at the middle and final LLM layers after training (Fig. 4, middle/right). Tokens from different tasks form well-separated clusters, indicating that HyperTokens learns distinct task characteristics while preserving previously acquired representations, thereby mitigating **Fog**.

Table 2: Contribution of loss terms on NExT-QA. \mathcal{L}_{Reg} comprises both $\mathcal{L}_{\text{LA-Reg}}$ and $\mathcal{L}_{\omega\text{-Reg}}$.

\mathcal{L}_{Ctr}	\mathcal{L}_{Reg}	$\mathcal{L}_{\text{Ques}}$	\mathcal{L}_{Vid}	\mathcal{L}_{Tok}	Acc (↑)	Fog (↓)
×	×	×	×	×	46.58	13.83
✓	×	×	×	×	57.83	6.39
✓	✓	×	×	×	59.47	5.95
✓	✓	✓	×	×	<u>62.77</u>	<u>4.98</u>
✓	✓	×	✓	×	60.52	5.52
✓	✓	×	×	✓	60.03	5.74
✓	✓	✓	✓	✓	64.75	3.62

Loss contribution We ablate the HyperTokens training objectives on NExT-QA, including the task-code contrastive loss \mathcal{L}_{Ctr} , the regularisers $\mathcal{L}_{\text{LA-Reg}}$ and $\mathcal{L}_{\omega\text{-Reg}}$, and the auxiliary terms listed in Table 2. The main gains come from \mathcal{L}_{Ctr} and the regularisers, which most directly reduce forgetting. For auxiliary losses, $\mathcal{L}_{\text{Ques}}$ is strongest, and among the two anti-causal surrogates, \mathcal{L}_{Vid} slightly outperforms \mathcal{L}_{Tok} .

Effect of look-ahead steps We vary the number of look-ahead updates in Eq. 4 from 0 to 2 and omit larger values due to compute limits. Table 3 shows that increasing the steps consistently improves both **Acc** and **Fog**, supporting the role of look-ahead updates in mitigating overfitting to the current task and reducing forgetting.

5.2. ImageQA \rightarrow VideoQA

5.2.1. SETUP

Dataset We use Visual7W (Zhu et al., 2016) (28,653 images; 139,868 QA pairs) as the ImageQA task and pair it with NExT-QA to construct alternating ImageQA/VideoQA continual sequences. We first pretrain offline on Visual7W, then continue on NExT-QA under the original 8-task sequential protocol, to assess how ImageQA pretraining affects downstream video reasoning during continual adaptation.

Baselines & Metrics To our knowledge, LLM-based PEA baselines have not been evaluated for this setting. We benchmark the second-best Bisecl and our HyperTokens by treating each image as a single-frame video and duplicating its visual tokens to match the video token length, enabling a unified continual fine-tuning protocol across tasks.

Implementation Details We follow the same backbone and hyperparameters as in our NExT-QA setup. On Visual7W, we fine-tune for ten epochs using \mathcal{L}_{NLL} and \mathcal{L}_{Ctr} . Since images do not require temporal reasoning, we retain only the question-level auxiliary loss $\mathcal{L}_{\text{Ques}}$ and disable video-specific ones. We use an 80/20 train-validation split.

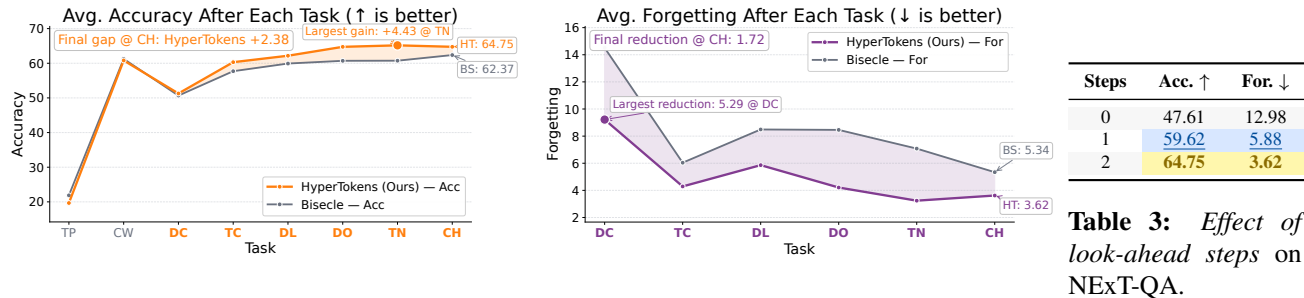


Figure 3: HyperTokens consistently surpasses Bisecle across tasks with higher average accuracy and lower average forgetting. We exclude TP and CW since forgetting happens only from DC onwards.

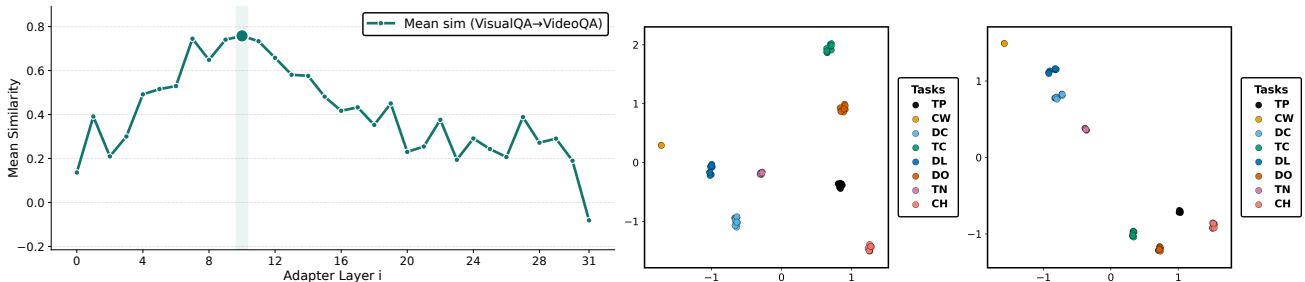


Figure 4: **Token analysis.** **Left:** Mean image–video token similarity across adapter layers after Visual7W→NEX-T-QA continual training. **Middle/Right:** t-SNE visualisations of token representations at representative mid and late layers after NEX-T-QA continual VideoQA training.

Table 4: Continual ImageQA → VideoQA results on Visual7W→NEX-T-QA, with accuracy and forgetting. **Bold** and **underline** denote the best and second-best results.

Method (Venue)	Visual7W		NEX-T-QA	
	Acc (↑)	Fog (↓)	Acc (↑)	Fog (↓)
Bisecle (NeurIPS’25)	38.21	30.35	55.32	6.31
HyperTokens (ours)	<u>45.59</u>	<u>26.11</u>	<u>60.07</u>	<u>4.97</u>

5.2.2. RESULTS

Table 4 shows HyperTokens clearly outperforms Bisecle on Visual7W→NEX-T-QA in both **Acc** and **Fog**. Importantly, continual ImageQA→VideoQA is harder than continual VideoQA alone and can induce negative transfer: Bisecle drops sharply (e.g., 62.37% → 55.32%), while HyperTokens degrades only mildly (4.68% accuracy).

We hypothesise this comes from a depth-wise mismatch: ImageQA pretraining strengthens shared mid-layer semantics, but introduces a static-scene bias and reduces late-layer plasticity needed for temporal reasoning. Our token analysis (Fig. 4 left) supports this: ImageQA and VideoQA prompt similarity peaks in the mid layers and then declines toward the final layers, where temporal specialisation emerges. To avoid freezing temporal learning, we disable forgetting constraints during transfer; even then, HyperTokens is more ro-

bust to the task switch, retaining over 7% higher Visual7W accuracy at the end of continual training.

6. Conclusion

We presented **HyperTokens**, a transformer-based token hyper-generator for continual VideoQA that synthesises fine-tuning tokens on demand, enabling *explicit, memory-bounded* adaptation with a fixed budget. To mitigate forgetting, we introduced a look-ahead regulariser that stabilises updates and anchors the generator to prior tasks, and we connected it to *sharpness-aware minimisation* to explain improved retention via flatter cross-task minima. Finally, guided by a causal view of VideoQA, we analysed feasible auxiliary objectives for token learning and proposed lightweight cross-modal supervision that strengthens alignment without inducing anti-causal drift.

While HyperTokens consistently improves accuracy and reduces forgetting on standard continual VideoQA, we observe mild negative transfer in the challenging ImageQA→VideoQA setting. Encouragingly, the degradation is smaller than that of a recent strong baseline, underscoring both the promise and the difficulty of cross-modal continual transfer. We view ImageQA→VideoQA as a benchmark for future work on connecting heterogeneous tasks, and hope HyperTokens provides a strong foundation towards more general lifelong learning across modalities.

Impact Statement

HyperTokens advances continual multimodal learning by closing a practical–theoretical gap in how we adapt large VideoQA models over time. Practically, it offers an explicit, memory-bounded mechanism to synthesise fine-tuning tokens on demand under a fixed budget, which can make continual deployment more feasible on resource-constrained systems. Theoretically, the look-ahead regulariser and its connection to sharpness-aware minimisation provide a principled explanation for improved retention via flatter cross-task minima, helping to clarify why and when such continual adaptation is stable.

Beyond the method itself, we highlight a challenging ImageQA→VideoQA continual transfer setting that reveals limitations of current approaches and provides a natural benchmark for bridging heterogeneous modalities. We position this setting as a stress test for cross-modal continual transfer, and show that HyperTokens incurs smaller degradation than a strong baseline, pointing to a concrete direction for building more general lifelong learners. In the longer term, memory-bounded continual adaptation, supported by carefully designed auxiliary supervision and robust anti-forgetting regularisation, can benefit real-world systems that learn from evolving visual streams, such as assistive agents, robotic perception, surveillance and safety monitoring, and interactive video understanding, while reducing catastrophic forgetting and cross-modal drift.

References

- Adhikari, S., Chandra, D. S., Srijith, P., Wasnik, P., and Oneo, N. Adaprefix++: Integrating adapters, prefixes and hypernetwork for continual learning. In *WACV*, pp. 7298–7307, 2025.
- Alayrac, J.-B., Donahue, J., Luc, P., Miech, A., Barr, I., Hasson, Y., Lenc, K., Mensch, A., Millican, K., Reynolds, M., et al. Flamingo: a visual language model for few-shot learning. *NeurIPS*, 35:23716–23736, 2022.
- Anil, R., Borgeaud, S., Wu, Y., Alayrac, J.-B., Yu, J., Soricut, R., Schalkwyk, J., Dai, A. M., et al. Gemini: A family of highly capable multimodal models. *arXiv preprint arXiv:2312.11805*, 2023.
- Benjamin, A. S., Rolnick, D., and Kording, K. Measuring and regularizing networks in function space. In *ICLR*, 2019.
- Buzzega, P., Boschini, M., Porrello, A., Abati, D., and Calderara, S. Dark experience for general continual learning: a strong, simple baseline. *NeurIPS*, 33:15920–15930, 2020.
- Cai, C., Wang, Z., Gao, J., Liu, W., Lu, Y., Zhang, R., and Yap, K.-H. Empowering large language model for continual video question answering with collaborative prompting. In *EMNLP*, 2024.
- Chandra, D. S., Varshney, S., Srijith, P., and Gupta, S. Continual learning with dependency preserving hypernetworks. In *WACV*, pp. 2339–2348, 2023.
- Charakorn, R., Cetin, E., Tang, Y., and Lange, R. T. Text-to-loRA: Instant transformer adaption. In *ICML*, 2025.
- Cheng, F., Wang, Z., Sung, Y.-L., Lin, Y.-B., Bansal, M., and Bertasius, G. Dam: Dynamic adapter merging for continual video qa learning. In *WACV*, 2025.
- Choi, S., On, K.-W., Heo, Y.-J., Seo, A., Jang, Y., Lee, M., and Zhang, B.-T. Dramaqa: Character-centered video story understanding with hierarchical qa. In *AAAI*, volume 35, pp. 1166–1174, 2021.
- Deitke, M., Clark, C., Lee, S., Tripathi, R., Yang, Y., Park, J. S., Salehi, M., Muennighoff, N., Lo, K., Soldaini, L., et al. Molmo and pixmo: Open weights and open data for state-of-the-art vision-language models. In *CVPR*, pp. 91–104, 2025.
- Dosovitskiy, A., Beyer, L., Kolesnikov, A., Weissenborn, D., Zhai, X., Unterthiner, T., Dehghani, M., Minderer, M., Heigold, G., Gelly, S., Uszkoreit, J., and Hounsby, N. An image is worth 16x16 words: Transformers for image recognition at scale. In *ICLR*, 2021.
- Foret, P., Kleiner, A., Mobahi, H., and Neyshabur, B. Sharpness-aware minimization for efficiently improving generalization. In *ICLR*, 2021.
- Gao, Q., Zhao, C., Sun, Y., Xi, T., Zhang, G., Ghanem, B., and Zhang, J. A unified continual learning framework with general parameter-efficient tuning. In *ICCV*, 2023.
- Gupta, G., Yadav, K., and Paull, L. Look-ahead meta learning for continual learning. *NeurIPS*, 33:11588–11598, 2020.
- Ha, D., Dai, A. M., and Le, Q. V. Hypernetworks. In *ICLR*, 2017.
- Hemati, H., Lomonaco, V., Bacciu, D., and Borth, D. Partial hypernetworks for continual learning. In *CoLLAs*, pp. 318–336. PMLR, 2023.
- Jha, S., Gong, D., and Yao, L. Clap4clip: Continual learning with probabilistic finetuning for vision-language models. *NeurIPS*, 37:129146–129186, 2024.
- Ke, Z., Liu, B., and Huang, X. Continual learning of a mixed sequence of similar and dissimilar tasks. *NeurIPS*, 33:18493–18504, 2020.

- Kirkpatrick, J., Pascanu, R., Rabinowitz, N., Veness, J., Desjardins, G., Rusu, A. A., Milan, K., Quan, J., Ramalho, T., Grabska-Barwinska, A., et al. Overcoming catastrophic forgetting in neural networks. *PNAS*, 114(13):3521–3526, 2017.
- Kumaravelu, V., Srijith, P., and Gupta, S. Evocl: Continual learning over evolving domains. In *WACV*, pp. 7533–7541, 2025.
- Lester, B., Al-Rfou, R., and Constant, N. The power of scale for parameter-efficient prompt tuning. In *EMNLP*, 2021.
- Li, X. L. and Liang, P. Prefix-tuning: Optimizing continuous prompts for generation. In *ACL*, 2021.
- Liu, A., Feng, B., Xue, B., Wang, B., Wu, B., Lu, C., Zhao, C., Deng, C., Zhang, C., Ruan, C., et al. Deepseek-v3 technical report. *arXiv preprint arXiv:2412.19437*, 2024a.
- Liu, H., Li, C., Li, Y., and Lee, Y. J. Improved baselines with visual instruction tuning. In *CVPR*, 2024b.
- Liu, H., Li, C., Wu, Q., and Lee, Y. J. Visual instruction tuning. In *NeurIPS*, volume 36, 2024c.
- Liu, W., Zhu, F., Wei, L., and Tian, Q. C-clip: Multimodal continual learning for vision-language model. In *ICLR*, 2025a.
- Liu, Y., Hong, Q., Huang, L., Gomez-Villa, A., Goswami, D., Liu, X., van de Weijer, J., and Tian, Y. Continual learning for vlms: A survey and taxonomy beyond forgetting. *arXiv preprint arXiv:2508.04227*, 2025b.
- Maaz, M., Rasheed, H., Khan, S., and Khan, F. Video-chatgpt: Towards detailed video understanding via large vision and language models. In *ACL*, pp. 12585–12602, 2024.
- McCloskey, M. and Cohen, N. J. Catastrophic interference in connectionist networks: The sequential learning problem. In *Psychology of learning and motivation*, volume 24. Elsevier, 1989.
- Nguyen, T., Do, K., Nguyen, D. T., Duong, B., and Nguyen, T. Causal inference via style transfer for out-of-distribution generalisation. In *KDD*, pp. 1746–1757, 2023.
- Nguyen, T., Kieu, D., Duong, B., Kieu, T., Do, K., Nguyen, T., and Le, B. Class-incremental learning with causal relational replay. *Expert Systems with Applications*, 250, 2024.
- Nichol, A., Achiam, J., and Schulman, J. On first-order meta-learning algorithms. *arXiv preprint arXiv:1803.02999*, 2018.
- Olsen, R. K., Moses, S. N., Riggs, L., and Ryan, J. D. The hippocampus supports multiple cognitive processes through relational binding and comparison. *Frontiers in human neuroscience*, 6, 2012.
- Oord, A. v. d., Li, Y., and Vinyals, O. Representation learning with contrastive predictive coding. *arXiv preprint arXiv:1807.03748*, 2018.
- Pearl, J. *Causality*. Cambridge university press, 2009.
- Qian, R., Dong, X., Zhang, P., Zang, Y., Ding, S., Lin, D., and Wang, J. Streaming long video understanding with large language models. *NeurIPS*, 37:119336–119360, 2024.
- Radford, A., Kim, J. W., Hallacy, C., Ramesh, A., Goh, G., Agarwal, S., Sastry, G., Askell, A., Mishkin, P., Clark, J., et al. Learning transferable visual models from natural language supervision. In *ICML*, pp. 8748–8763, 2021.
- Razdaibiedina, A., Mao, Y., Hou, R., Khabsa, M., Lewis, M., and Almahairi, A. Progressive prompts: Continual learning for language models. In *ICLR*, 2023.
- Riemer, M., Cases, I., Ajemian, R., Liu, M., Rish, I., Tu, Y., and Tesauro, G. Learning to learn without forgetting by maximizing transfer and minimizing interference. In *ICLR*, 2019.
- Rusu, A. A., Rabinowitz, N. C., Desjardins, G., Soyer, H., Kirkpatrick, J., Kavukcuoglu, K., Pascanu, R., and Hadsell, R. Progressive neural networks. *arXiv preprint arXiv:1606.04671*, 2016.
- Shu, F., Zhang, L., Jiang, H., and Xie, C. Audio-visual llm for video understanding. In *ICCV*, pp. 4246–4255, 2025.
- Smith, J. S., Karlinsky, L., Gutta, V., Cascante-Bonilla, P., Kim, D., Arbelle, A., Panda, R., Feris, R., and Kira, Z. Coda-prompt: Continual decomposed attention-based prompting for rehearsal-free continual learning. In *CVPR*, 2023.
- Tan, Y., Hu, X., Xue, H., De Melo, C., and Salim, F. D. Bisecl: Binding and separation in continual learning for video language understanding. *NeurIPS*, 2025a.
- Tan, Z., Zhang, Z., Wen, H., Li, Z., Zhang, R., Chen, P., Mo, F., Liu, Z., Zeng, Q., Yin, Q., et al. Instant personalized large language model adaptation via hypernetwork. *arXiv preprint arXiv:2510.16282*, 2025b.

- Team, G., Georgiev, P., Lei, V. I., Burnell, R., Bai, L., Gulati, A., Tanzer, G., Vincent, D., Pan, Z., Wang, S., et al. Gemini 1.5: Unlocking multimodal understanding across millions of tokens of context. *arXiv preprint arXiv:2403.05530*, 2024.
- Touvron, H., Martin, L., Stone, K., Albert, P., Almahairi, A., Babaei, Y., Bashlykov, N., Batra, S., Bhargava, P., Bhosale, S., et al. Llama 2: Open foundation and fine-tuned chat models. *arXiv preprint arXiv:2307.09288*, 2023.
- von Oswald, J., Henning, C., Grewe, B. F., and Sacramento, J. Continual learning with hypernetworks. In *ICLR*, 2020.
- Wang, L., Xie, J., Zhang, X., Huang, M., Su, H., and Zhu, J. Hierarchical decomposition of prompt-based continual learning: Rethinking obscured sub-optimality. *NeurIPS*, 2023.
- Wang, Z., Zhang, Z., Ebrahimi, S., Sun, R., Zhang, H., Lee, C.-Y., Ren, X., Su, G., Perot, V., Dy, J., et al. Dualprompt: Complementary prompting for rehearsal-free continual learning. In *ECCV*, 2022a.
- Wang, Z., Zhang, Z., Lee, C.-Y., Zhang, H., Sun, R., Ren, X., Su, G., Perot, V., Dy, J., and Pfister, T. Learning to prompt for continual learning. In *CVPR*, 2022b.
- Xiao, J., Shang, X., Yao, A., and Chua, T.-S. Next-qa: Next phase of question-answering to explaining temporal actions. In *CVPR*, pp. 9777–9786, 2021.
- Yang, A., Miech, A., Sivic, J., Laptev, I., and Schmid, C. Zero-shot video question answering via frozen bidirectional language models. *NeurIPS*, 35:124–141, 2022.
- Yu, J., Huang, Z., Zhuge, Y., Zhang, L., Hu, P., Wang, D., Lu, H., and He, Y. Moe-adapters++: Towards more efficient continual learning of vision-language models via dynamic mixture-of-experts adapters. *TPAMI*, 2025.
- Yu, S., Cho, J., Yadav, P., and Bansal, M. Self-chained image-language model for video localization and question answering. *NeurIPS*, 36:76749–76771, 2023.
- Zenke, F., Poole, B., and Ganguli, S. Continual learning through synaptic intelligence. In *ICML*, pp. 3987–3995. PMLR, 2017.
- Zhang, C., Lu, T., Islam, M. M., Wang, Z., Yu, S., Bansal, M., and Bertasius, G. A simple llm framework for long-range video question-answering. In *EMNLP*, pp. 21715–21737, 2024a.
- Zhang, R., Han, J., Liu, C., Zhou, A., Lu, P., Qiao, Y., Li, H., and Gao, P. LLaMA-adapter: Efficient fine-tuning of large language models with zero-initialized attention. In *ICLR*, 2024b.
- Zhao, H., Ni, B., Fan, J., Wang, Y., Chen, Y., Meng, G., and Zhang, Z. Continual forgetting for pre-trained vision models. In *CVPR*, pp. 28631–28642, 2024.
- Zhu, Y., Groth, O., Bernstein, M., and Fei-Fei, L. Visual7w: Grounded question answering in images. In *CVPR*, pp. 4995–5004, 2016.

A. Extended Preliminaries

A.1. LLaMA-Adapter.

Following prior work (Tan et al., 2025a; Cai et al., 2024), we adopt *LLaMA-Adapter* (Zhang et al., 2024b) for parameter-efficient continual adaptation of a frozen multimodal LLM backbone on VideoQA. For each task t , we introduce a small set of adapter tokens at selected Transformer layers, $P_l^t \in \mathbb{R}^{N_p^t \times C}$, $l = 1, \dots, L_{\text{adapter}}$, which are injected into the frozen backbone and optimised under the main objective in Eq. 3. In our framework, the token generator H_ϕ synthesises $\{P_l^t\}$ conditioned on task codes extracted by g_ω ; we therefore primarily optimise ϕ (and ω) during continual fine-tuning.

Unimodal adapter injection via KV-prefix attention. Let $Q_l \in \mathbb{R}^{N_q^t \times C}$ denote the layer- l hidden states of the text question sequence. We augment the keys/values with adapter tokens:

$$\tilde{Q}_l = [P_l^t; Q_l] \in \mathbb{R}^{(N_p^t + N_q^t) \times C}, \quad (18)$$

and apply attention with queries from Q_l and keys/values from \tilde{Q}_l :

$$\text{Attn}(Q_l, \tilde{Q}_l) = \text{softmax}\left(\frac{(Q_l W_Q)(\tilde{Q}_l W_K)^\top}{\sqrt{d_h}}\right) (\tilde{Q}_l W_V), \quad (19)$$

where d_h denotes the per-head dimension (we omit the multi-head notation for clarity). This is followed by the standard residual update (and FFN as usual):

$$Q'_l = Q_l + \text{Attn}(Q_l, \tilde{Q}_l), \quad Q_{l+1} = Q'_l + \text{FFN}(Q'_l). \quad (20)$$

This yields a lightweight adaptation while keeping the pretrained backbone frozen. However, in the multimodal setting of VideoQA, we must also adapt the visual stream; next, we describe how we integrate and adapt video inputs for LLaMA.

Multimodal adapter via feature projection. Given a visual input (video or image), we extract visual tokens $V^t \in \mathbb{R}^{N_v^t \times C_{\text{vis}}}$ and project them to the LLaMA width with a lightweight projector $W_{\text{vis}}^t \in \mathbb{R}^{C_{\text{vis}} \times C}$:

$$V_0^t = V^t W_{\text{vis}}^t \in \mathbb{R}^{N_v^t \times C}. \quad (21)$$

At layer l , let $X_l \in \mathbb{R}^{(N_v^t + N_q^t) \times C}$ denote the joint hidden sequence obtained by inserting the current visual-token slice V_l^t into the reserved visual slots of the text stream (thus V_l^t evolves across layers as part of X_l). We then apply the same KV-prefix attention with adapter tokens:

$$X'_l = X_l + \text{Attn}(X_l, [P_l^t; X_l]), \quad X_{l+1} = X'_l + \text{FFN}(X'_l). \quad (22)$$

B. Theoretical Results

B.1. Proof for Theorem 4.1

Before presenting the proof, we briefly recall the intuition behind *Sharpness-Aware Minimisation* (SAM) (Foret et al., 2021) and its benefits in domain generalisation.

SAM and Domain Generalisation. Given a loss function $\mathcal{L}(\theta)$, SAM optimises the robust objective

$$\min_{\theta} \max_{\|\epsilon\| \leq \rho} \mathcal{L}(\theta + \epsilon), \quad (23)$$

which seeks parameters whose loss remains small under worst-case perturbations within a local neighbourhood of radius ρ . Under a first-order approximation, the inner maximisation admits the solution $\epsilon^* = \rho \nabla_{\theta} \mathcal{L}(\theta) / \|\nabla_{\theta} \mathcal{L}(\theta)\|$, leading to updates that penalise directions of high curvature. Such solutions correspond to flatter minima, which are known to exhibit improved generalisation under distribution or domain shift. This robustness perspective provides the key intuition for LA-Reg, whose objective can be interpreted as enforcing prediction consistency under a lookahead parameter perturbation.

Proof. Fix any previous task index $\tau < t$. For brevity, let

$$H_\phi^\tau \triangleq H_\phi(z^\tau), \quad J_\phi^\tau \triangleq J_\phi(z^\tau),$$

and define

$$a_\tau \triangleq H_\phi^\tau - H_{\phi^*}^\tau, \quad b_\tau \triangleq J_\phi^\tau \Delta\phi.$$

By Assumption (A1 – Smoothness of the token generator), for each $\tau < t$ the second-order expansion yields

$$H_{\phi+\Delta\phi}^\tau = H_\phi^\tau + J_\phi^\tau \Delta\phi + r_\tau = H_\phi^\tau + b_\tau + r_\tau,$$

where $\|r_\tau\|_2 \leq C_H \|\Delta\phi\|_2^2$. It follows that

$$H_{\phi+\Delta\phi}^\tau - H_{\phi^*}^\tau = (H_\phi^\tau - H_{\phi^*}^\tau) + b_\tau + r_\tau = a_\tau + b_\tau + r_\tau. \quad (24)$$

Substituting this expression into the definition of $\mathcal{L}_{\text{LA-Reg}}^t$ in Eq. (16), we obtain

$$\mathcal{L}_{\text{LA-Reg}}^t(\phi) = \sum_{\tau=1}^{t-1} \|a_\tau + b_\tau + r_\tau\|_2^2. \quad (25)$$

Recall that $\Delta\phi = -\eta g(\phi)$. Hence, for each $\tau < t$,

$$b_\tau = J_\phi^\tau \Delta\phi = -\eta J_\phi^\tau g(\phi), \quad \text{and} \quad \|b_\tau\|_2^2 = \eta^2 \|J_\phi^\tau g(\phi)\|_2^2.$$

Therefore the leading contribution is precisely

$$\sum_{\tau=1}^{t-1} \|b_\tau\|_2^2 = \eta^2 \sum_{\tau=1}^{t-1} \|J_\phi(z^\tau) g(\phi)\|_2^2. \quad (26)$$

Returning to $\mathcal{L}_{\text{LA-Reg}}^t(\phi)$, we expand the squared norm for each τ :

$$\|a_\tau + b_\tau + r_\tau\|_2^2 = \|b_\tau\|_2^2 + \|a_\tau\|_2^2 + \|r_\tau\|_2^2 + 2\langle a_\tau, b_\tau \rangle + 2\langle a_\tau, r_\tau \rangle + 2\langle b_\tau, r_\tau \rangle.$$

Subtracting $\|b_\tau\|_2^2$ and summing over $\tau = 1, \dots, t-1$ gives

$$\mathcal{L}_{\text{LA-Reg}}^t(\phi) - \sum_{\tau=1}^{t-1} \|b_\tau\|_2^2 = \sum_{\tau=1}^{t-1} \left(\|a_\tau\|_2^2 + \|r_\tau\|_2^2 + 2\langle a_\tau, b_\tau \rangle + 2\langle a_\tau, r_\tau \rangle + 2\langle b_\tau, r_\tau \rangle \right). \quad (27)$$

Taking absolute values and applying Cauchy–Schwarz inequality, $|\langle u, v \rangle| \leq \|u\|_2 \|v\|_2$, we obtain

$$\left| \mathcal{L}_{\text{LA-Reg}}^t(\phi) - \sum_{\tau=1}^{t-1} \|b_\tau\|_2^2 \right| \leq \sum_{\tau=1}^{t-1} \left(\|a_\tau\|_2^2 + \|r_\tau\|_2^2 + 2\|a_\tau\|_2 \|b_\tau\|_2 + 2\|a_\tau\|_2 \|r_\tau\|_2 + 2\|b_\tau\|_2 \|r_\tau\|_2 \right). \quad (28)$$

We now bound each factor using the assumptions.

Bound on $\|a_\tau\|_2$. By (A2 – Reference proximity), for all $\tau < t$,

$$\|a_\tau\|_2 = \|H_\phi(z^\tau) - H_{\phi^*}(z^\tau)\|_2 \leq \varepsilon.$$

Bounds on $\|b_\tau\|_2$ and $\|r_\tau\|_2$. From (A1 - Smoothness of the token generator) and (A3 – Bounded current-task gradient),

$$\|b_\tau\|_2 = \|J_\phi^\tau \Delta\phi\|_2 \leq \|J_\phi^\tau\| \|\Delta\phi\|_2 \leq L_J \cdot \eta \|g(\phi)\|_2 \leq L_J \eta G.$$

Also, using $\|r_\tau\|_2 \leq C_H \|\Delta\phi\|_2^2$ from (A1 – Smoothness of the token generator) and $\|\Delta\phi\|_2 = \eta \|g(\phi)\|_2 \leq \eta G$,

$$\|r_\tau\|_2 \leq C_H (\eta G)^2 = C_H \eta^2 G^2, \quad \|r_\tau\|_2^2 \leq C_H^2 \eta^4 G^4.$$

Plugging these bounds into Eq. (28), for each τ we get

$$\left| \mathcal{L}_{\text{LA-Reg}}^t(\phi) - \sum_{\tau=1}^{t-1} \|b_\tau\|_2^2 \right| \leq \sum_{\tau=1}^{t-1} \left(\varepsilon^2 + 2L_J G \varepsilon \eta + 2C_H G^2 \varepsilon \eta^2 + 2C_H L_J G^3 \eta^3 + C_H^2 G^4 \eta^4 \right). \quad (29)$$

We choose the update rate η sufficiently small so that $\eta \leq 1$, then $\eta^2 \leq \eta$ and $\eta^4 \leq \eta^3$. Applying these inequalities in Eq. (29) yields $\varepsilon \eta^2 \leq \varepsilon \eta$, and $\eta^4 \leq \eta^3$. Then we have

$$\left| \mathcal{L}_{\text{LA-Reg}}^t(\phi) - \sum_{\tau=1}^{t-1} \|b_\tau\|_2^2 \right| \leq (t-1) \left(\varepsilon^2 + (2L_J G + 2C_H G^2) \varepsilon \eta + (2C_H L_J G^3 + C_H^2 G^4) \eta^3 \right). \quad (30)$$

Define the constant $C := (t-1) \max \left\{ 1, 2L_J G + 2C_H G^2, 2C_H L_J G^3 + C_H^2 G^4 \right\}$ which is independent of η . Then Eq. (30) implies

$$\left| \mathcal{L}_{\text{LA-Reg}}^t(\phi) - \sum_{\tau=1}^{t-1} \|b_\tau\|_2^2 \right| \leq C(\varepsilon^2 + \varepsilon \eta + \eta^3). \quad (31)$$

Finally, substituting Eq. (26) (i.e., $\sum_{\tau < t} \|b_\tau\|_2^2 = \eta^2 \sum_{\tau < t} \|J_\phi(z^\tau)g(\phi)\|_2^2$) gives exactly Eq. (17). This completes the proof. \square

C. Additional Experimental Details

C.1. Architecture

g_ω implementation. We implement g_ω as a lightweight multimodal encoder that maps each sample (V_i^t, Q_i^t) to a fixed-length token sequence $\tilde{z}_i^t \in \mathbb{R}^{N_z \times C_z}$ (we use $N_z=32, C_z=256$). We linearly project V_i^t and Q_i^t to width C_z , add learned modality/type embeddings, and apply residual depthwise-separable 1D convolutions for local temporal/context mixing. The two streams are then concatenated and fused by a small pre-norm Transformer encoder (self-attention + FFN; 2 layers, 4 heads, dropout 0.2) with padding masks. Finally, we pool the variable-length fused sequence into exactly N_z tokens using learned pooling queries with a cross-attention pooling layer, yielding $\tilde{z}_i^t = g_\omega(V_i^t, Q_i^t)$ for task-code learning and prototype-based contrastive supervision.

H_ϕ implementation. We follow the transformer-based architecture described in the main paper for H_ϕ . In our implementation, the token generator produces at most $N_p=32$ prompt tokens with hidden width $C_p=256$ across both datasets. The Transformer uses 4 layers with 8 attention heads and dropout 0.2 (for both NExT-QA and DramaQA).

C.2. Hyper-parameters and Continual Fine-tuning Details

Training schedule. We fine-tune for five epochs on NExT-QA and ten epochs on the other datasets, always with a two-epoch warm-up, using NVIDIA H200 GPUs. Our method updates more trainable components rather than a small shared prompt, and therefore typically requires a longer optimisation horizon to reach a stable solution. To keep comparisons fair, we report baseline results using the training budgets specified in their original papers; in addition, we confirmed that increasing baseline training to ten epochs does not yield further gains, indicating that five epochs are already sufficient for their convergence.

Optimiser and batching. We use AdamW with $(\beta_1, \beta_2) = (0.9, 0.95)$. On NExT-QA, we use per-GPU batch size 4 with gradient accumulation of 16 steps. On DramaQA, we use per-GPU batch size 4 with gradient accumulation of 32 steps. We fix the random seed to 42 for all experiments.

Learning rates. We use a smaller learning rate for g_ω and the token generator H_ϕ than for other trainable modules. On NExT-QA, we set $\text{lr}(g_\omega) = \text{lr}(H_\phi) = 10^{-3}$ and use 5×10^{-3} for all remaining modules. On DramaQA, we set $\text{lr}(g_\omega) = \text{lr}(H_\phi) = 10^{-4}$ while keeping the other modules at 5×10^{-3} .

Table 5: Fine-tuning hyper-parameters.

Setting	NExT-QA	DramaQA
Epochs (warm-up)	5 (2)	10 (2)
Batch size / GPU	4	4
Grad. accumulation	16	32
Optimiser	AdamW	AdamW
(β_1, β_2)	(0.9, 0.95)	(0.9, 0.95)
Weight decay	0.14	0.10
Seed	42	42

Table 6: Loss weights, temperatures, and look-ahead settings.

Hyper-parameter	Value	Applies to
$\alpha_{\text{LA-Reg}}$	0.25	all datasets
$\alpha_{\omega\text{-Reg}}$	5000	all datasets
α_{Ctr}	0.5	all datasets
α_{Vid}	0.1	auxiliary loss
α_{Tok}	0.1	auxiliary loss
α_{Ques}	1.0	auxiliary loss
ρ_{Vid}	0.01	\mathcal{L}_{Vid}
ρ_{Tok}	100	\mathcal{L}_{Tok}
Look-ahead step size	$0.5 \times$ base lr	inner loop
Look-ahead steps	2	inner loop

Loss weights and temperatures. We set $\alpha_{\text{LA-Reg}} = 0.25$ and $\alpha_{\text{Ctr}} = 0.5$ for both datasets. We set $\alpha_{\omega\text{-Reg}} = 5000$; in practice we scale $\mathcal{L}_{\omega\text{-Reg}}$ by the number of parameters in g_{ω} to prevent numerical overflow. For auxiliary supervision, we weight \mathcal{L}_{Vid} and \mathcal{L}_{Tok} by 0.1, and $\mathcal{L}_{\text{Ques}}$ by 1.0, as the question-prediction signal is consistently more effective.

We use temperature $\rho_{\text{Vid}} = 0.01$ in \mathcal{L}_{Vid} and $\rho_{\text{Tok}} = 100$ in \mathcal{L}_{Tok} . A small ρ_{Vid} sharpens discrimination between positive and negative videos, which are typically distinct; in contrast, token positives/negatives can be semantically related, where a softer distribution (larger temperature) is beneficial.

Look-ahead update. For the look-ahead inner loop, we use a step size equal to $0.5 \times$ the base learning rate with 2 inner steps in total by default.

We summarise fine-tuning hyper-parameters on NExT-QA and DramaQA in Tables 5 and 6.

Pretraining on Visual7W. For the Visual7W \rightarrow NExT-QA transfer setting, we pretrain both Bisecl and HyperTokens for 10 epochs with a 2-epoch warm-up. We use AdamW with batch size 16 and gradient accumulation of 64. For HyperTokens, we set the learning rates of g_{ω} and H_{ϕ} to 5×10^{-4} , and use 5×10^{-3} for all other modules; Bisecl also uses 5×10^{-3} . All remaining hyperparameters follow the NExT-QA setup to ease transfer. We select the checkpoint with the best validation accuracy for subsequent continual adaptation on VideoQA.

D. Extended Related Work

Image Question Answering (ImageQA) ImageQA is a core multimodal task that requires models to understand visual content and produce accurate natural-language answers. Recent advances in multimodal LLMs have substantially improved ImageQA performance (Anil et al., 2023; Liu et al., 2024c). However, most VQA systems are trained offline and do not address continual learning from evolving multimodal data, as required in practice and in VideoQA. Moreover, their ability to transfer under continual adaptation to the more challenging continual VideoQA setting remains largely untested.

Meta Learning for Continual Learning Meta-learning mitigates forgetting by optimising parameters (or update rules) for rapid adaptation with minimal interference. Existing meta-CL methods largely focus on optimisation objectives that promote transfer, e.g., MER encourages gradient alignment across replayed experiences via Reptile-style updates (Nichol et al., 2018; Riemer et al., 2019), and La-MAML brings a look-ahead objective with per-parameter learning-rate modulation to the online-continual regime (Gupta et al., 2020). We instead target a more challenging setting—prompt-based continual adaptation for multimodal video reasoning—where our look-ahead term regularises the *prompt space* (rather than directly shaping gradients) and is theoretically connected to sharpness-aware minimisation, bridging meta-learning, generalisation, and continual learning.

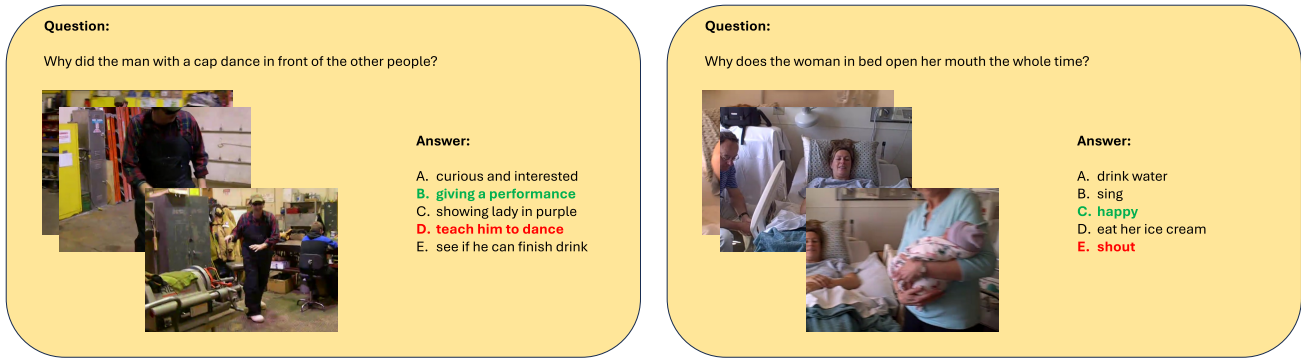


Figure 5: **Qualitative Examples 1–2.** HyperTokens predicts the correct answer (green), whereas Bisecler produces an incorrect one (red) in continual VideoQA.



Figure 6: **Qualitative Examples 3–4.** HyperTokens predicts the correct answer (green), whereas Bisecler produces an incorrect one (red) in continual VideoQA.

E. Qualitative Results

E.1. Continual VideoQA

Fig. 5 and Fig. 6 present qualitative comparisons in continual VideoQA. HyperTokens consistently yields the correct answer, whereas Bisecler fails in these cases.

E.2. ImageQA→VideoQA transfer

Fig. 7 show qualitative results for continual ImageQA→VideoQA transfer. After adapting to video tasks, HyperTokens still predicts the correct answer, whereas Bisecler fails on these Visual7W examples.

F. More Ablation Studies and Analysis

Table 7: Performance with different numbers of prompt layers.

# P. Layer	Acc (↑)	Fog (↓)
8	54.12	8.79
16	58.45	6.08
24	59.92	5.65
32	64.75	3.62

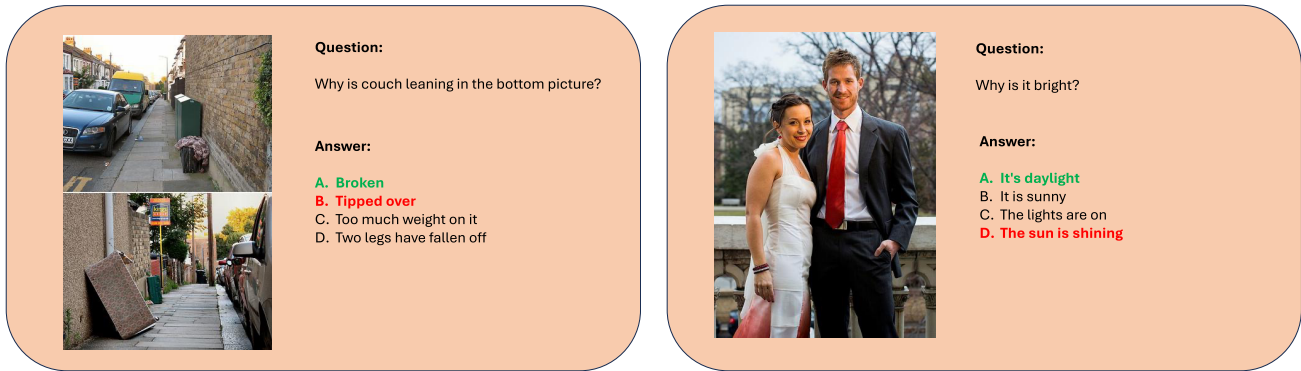


Figure 7: **Qualitative Examples 5–6.** After adapting to video tasks, HyperTokens still predicts the correct answer (green), whereas Bisele fails on these Visual7W examples (red).

F.1. Sensitivity to the Number of Prompt-Injection Layers

We study how HyperTokens varies with the number of adapted adapter layers in Table 7. Overall, increasing the adapted depth consistently improves performance, supporting the effectiveness of parameter-efficient adaptation for continual VideoQA.

F.2. Task Order

We evaluate HyperTokens under different task orders on NEX-T-QA and compare against Bisele in Table 8. HyperTokens is more robust, outperforming Bisele on three orders while remaining competitive on the fourth, supporting the effectiveness of multimodal token hyper-generation.

Table 8: Robustness to task order on NEX-T-QA: Bisele versus HyperTokens, reporting average accuracy and forgetting across four task permutations.

Task Order	Acc (↑)		Fog (↓)	
	Bisele	HyperTokens	Bisele	HyperTokens
<TP, TN, CH, TC, DL, DO, CW, DC>	57.98	59.52	7.16	6.52
<DO, CW, DC, CH, TP, TC, TN, DL>	57.95	60.03	8.93	6.84
<CW, DO, TN, DL, TC, TP, DC, CH>	62.25	62.73	5.70	4.98
<CH, DL, TP, TC, DC, DO, TN, CW>	63.09	62.91	2.87	3.16